

Dynamic analysis of train-bridge system under one-way and two-way high-speed train passing

Meysam Jahangiri* and Jabar-Ali Zakeri^a

School of Railway Engineering, Iran University of Science and Technology, Narmak, Tehran, Iran

(Received April 10, 2017, Revised June 20, 2017, Accepted July 4, 2017)

Abstract. In this paper, the dynamic responses of train-bridge system under one-way and two-way high-speed train passing are studied. The 3D finite element modeling is used and the bridge and train are modeled considering their details. The created model is validated by the results of the dynamic field test. To study the effect of train speed, different train passing scenarios are analyzed, including one-way passing, two-way passing in different directions at same speeds, and two-way passing in different directions at different speeds. The results show that the locations of maximum acceleration are different in one-way and two-way passing modes, and the maximum values in two-way passing mode are higher than those in one-way passing mode, while the maximum accelerations in both modes are almost identical. The displacement and acceleration values in different scenarios show peaks at speeds of 260 and 120 km/h, due to the proximity of the natural frequencies of the bridge and loading frequencies of the train at these speeds.

Keywords: dynamic interaction; high-speed train; 3D finite element modeling; two-way passing; dynamic field test

1. Introduction

Today, the use of rail transportation system has been accepted as one of the best transportation methods in the most developed countries. In these countries, high-speed trains play a major role in transportation management and are always in the center of attention. One of the important structures in the railroad are bridges that are constructed with different length and spans over the rail routes and make the traffic of the rail vehicles possible with acceptable quality. To provide the high-speed trains passing through bridges at the same time, bridges located in the high-speed railways are mostly two-lane. These bridges should be investigated accurately due to the high traffic load compared to the one-lane bridges as well as the effects of some factors such as the difference in the loading frequency caused by passing trains with different speeds.

Between the two world wars, the dynamics of railway bridges drew a great deal of attention in the former Soviet Union and Britain. During this time, Inglis (1934), theoretically and practically, described the effect of railway locomotives on the vibrations of the bridges. Delgado and Santos (1997) examined the effect of parameters such as stiffness and weight of the bridge, the rigidity of the vehicle, bridge span and rail surface roughness on the interaction of the bridge and the train using a simple two-dimensional model of the bridge-train interaction. Wu and Dai (1987) applied finite element method (FEM) to

investigate the effect of passing loads on simply-supported multi-span bridges. At first, they studied the effect of two moving loads in opposite directions followed by investigating the effect of passing loads through the effect of passing speed on the rate of displacement within the bridge span. Liu *et al.* (2009) studied the interaction between the bridge and the passing trains using a 2D FEM, where they considered the bridge as a simply-supported beam, ignored rotational degrees of freedom of the vehicle, and assumed the axle load constant along all axes. Xia *et al.* (2007) evaluated the dynamic responses of a suspension bridge under train passage using a FEM modeling and considered the effects of dynamic interaction in their model. These researchers also considered the contact of load and bridge as a point and assumed the viscoelastic features of materials as constant. Vesali *et al.* (2013) conducted an analytical study on the dynamic response of railway bridges traversed simultaneously by opposing moving trains. In this model, evaluation of the bridge-train interaction was impossible since loading the train was performed using moving loads. The bridge was assumed as a simply-supported beam and both sets of loads were passed through the beam; therefore, the evaluation of the torsion effect on the bridge was impossible. Sua *et al.* (2010) measured the dynamic responses of a 40-year-old viaduct under Japanese high-speed train passage (Shinkansen) using field measurements and numerical simulations. The results of acceleration and displacement of the bridge were recorded under high-speed train passage and used to validate the numerical model. In this study, the bridge was modeled and analyzed with the finite element ABAQUS software. The structural members incorporated into the bridge, such as foundations, beams, and sleepers were modeled with beam elements, but the bridge deck was modeled with shell elements. However, in this model, the interaction of the

*Corresponding author, Ph.D. Student

E-mail: m_jahangiri@rail.iust.ac.ir

^aProfessor

E-mail: Zakeri@iust.ac.ir

components of the superstructure was not taken into the account. Xia, Zhang and Gao (2005) performed some field measurements to evaluate the responses of a simply-supported PC girders railway bridge under high-speed train. The China-Star high-speed train was passing over the bridge at a speed of 120 to 350 km/h. The results of this research revealed that this bridge had satisfactory resistance and the vehicle stability parameters were within allowable limits. Xia and Nan Zhang (2005) conducted a numerical modeling and parametric analysis on a railway bridge subjected to high-speed trains. They also carried out a parametric analysis on passing speed and presented the results of acceleration and displacement from different points of the bridge and train. Dinh *et al.* (2009) proposed a simulation procedure for vehicle-substructure dynamic interactions and wheel movements. They considered each vehicle as a multi-axle two layer of mass-spring-damper system having 27 degrees of freedom. In another study by Dinh *et al.* (2009), a three-dimensional two-span continuous bridge with ballast superstructure is modelled. The bridge had a span length of 40m, and a one-way passing scenario was considered for trains. The model was validated by comparing the results with analytical solution of a simply supported bridge under a moving sprung mass. Xia *et al.* (2012) dynamically evaluated a coupled high-speed train and bridge system. The studied bridge was a simple span box girders bridge with a span length of 32 m. The results showed that the rail roughness was significantly effective on dynamic responses of the bridge. Moreover, it was demonstrated that an increase in rail roughness resulted in a decrease in critical speed in terms of travel comfort aspects. Xia *et al.* (2014) investigated the dynamic response of a train-bridge system under collision loads. In this study, the bridge was a concrete box girder high-speed railway bridge with simple span. The results showed that collision loads with a short pulse and higher loading rate had a greater effect on the response of the bridge. In addition, the bridge roughness with collision origin had greater effects on the response of vehicle and its stability criteria. Adam and Salcher (2014) studied the dynamic effect of high-speed trains on the simple bridge structures. They evaluated the dynamic responses of single-span, two-span, and continual-span simply supported bridges for some transitional loading along the passing train axles. They also evaluated the maximum values of dynamic response of the bridge. Naeimi *et al.* (2015) developed a mathematical model of the vehicle-track interaction to investigate the coupled behaviour of vehicle-track system, in the presence of uneven irregularities at left/right rails. The railway vehicle was simplified as a 3D multi-rigid-body model, and the track was treated as the two parallel beams on a layered discrete support system. Podworna (2014) evaluated the random dynamic analysis of the steel-concrete bridges subjected to high-speed train according to ICE-3 standard in Germany. In this study, the bridge had continual-span with ballistic superstructure and the train had two bogies at each wagon. The results showed that the effect of rail surface roughness on dynamic responses of bridge increased by increasing the spans of the bridge. Yan *et al.* (2015) conducted a comprehensive review of the prevalence of

high-speed railway bridge in the leading countries of this field. They compared the structural system of high-speed railway bridges as well as their bridge seats with each other and determined that the most common type of railway bridges is concrete box girders with a simple span and a span length less than 30 m. Li *et al.* (2015) presented a method for the non-destructive monitoring of high-speed railway bridge using strain results in some points of bridge subjected to the high-speed train passing. They divided the obtained strain results into two parts; force vibration and free vibration. The strain was identified in the analytical model by evaluation of strain results of critical values in the force vibration. Moreover, the strain mode shapes were derived by evaluation of strain results in free vibration part. Ugarte *et al.* (2017) investigated the dynamic responses of pergola bridge deck subjected to passing loads. They, firstly implemented a simple analytical method was employed to evaluate the complex dynamic behavior of such bridge followed by comparing the results of a simple analytic model with those of complex FEM, whereby they showed the acceptable precision of the analytical model.

The majority of studies conducted in the field of bridge-train interaction are associated with simplifying assumptions. However, considering the importance of high-speed railway bridges, these bridges need a higher precision control. In this paper, a two-lane bridge system and a high-speed train, as well as the interactions between them, are modeled accurately. In this 3D modeling, the effect of passing speed is evaluated in different passing scenarios including one-way passing, two-way passing in different directions and at the same speed, and two-way passing in different directions and various speeds. Finally, the values of critical speed are determined in different scenarios.

2. Research methodology

In the present study, a 3D FE model is employed in Abaqus finite element software to model and analyze the bridge and train while considering the interaction between them using the Hertz theory (Bhaskar, Johnson, Wood and Woodhouse 1997). Next, this model is validated by comparing the displacements and modal frequencies obtained from the numerical model and the field test. The numerical model is then used to assess sensitivity analysis.

The assumptions considered in this study are as follows:

- Train and bridge modeling is performed using the FEM.
- Each 4-axis vehicle is described by 27 degrees-of-freedom.
- The considered bridge is a two-lane simple span structure with concrete box girder system and Superstructure is concrete slab.
- Rails and springs-dampers related to pad and fastener are modeled.
- Train passes the bridge with different speeds (120 to 350 km/h).
- Moving train is considered as one-way and two-way passing mode.

The considered purposes of this research are as follows:

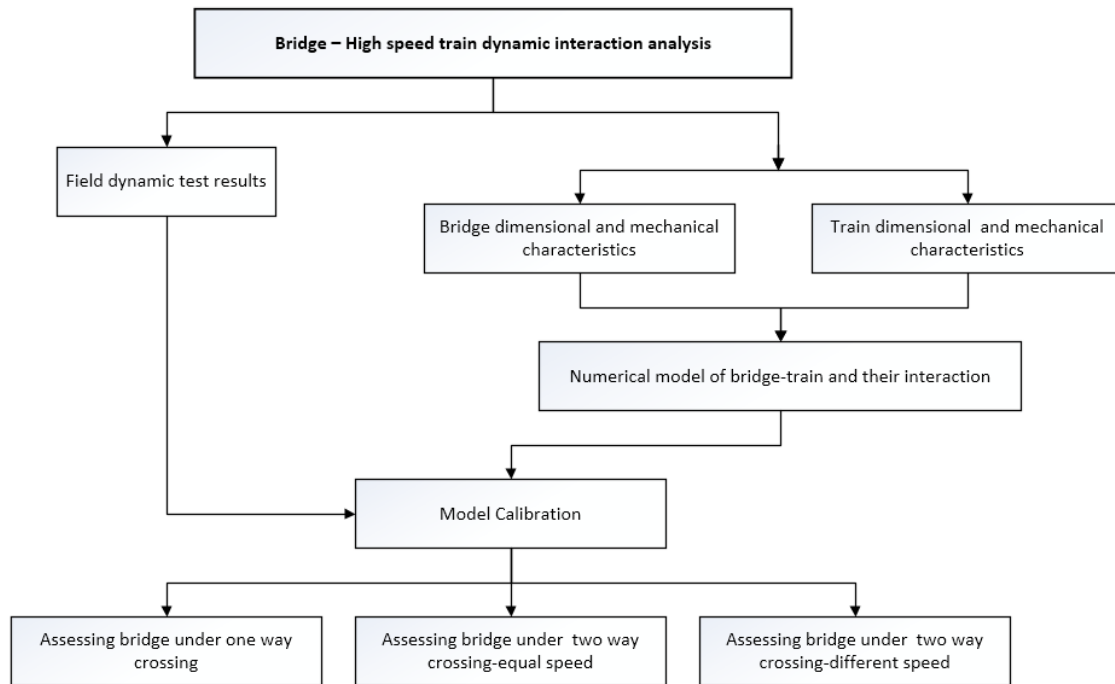


Fig. 1 Schematic methodology of the research

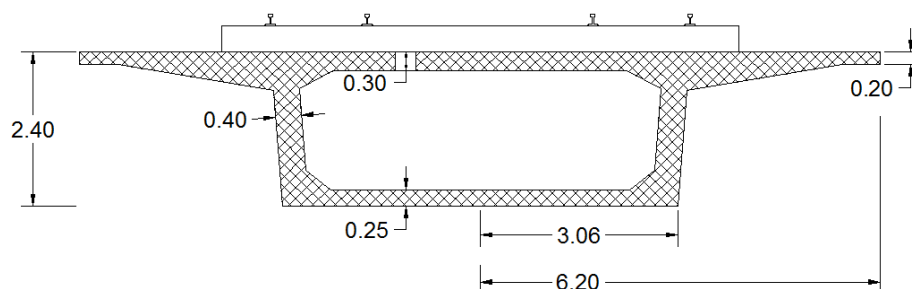


Fig. 2 Cross section of the 24-m-span PC box girder

- Controlling the speed effect of high-speed train on the results of the bridge in one-way passing mode and determining the critical speeds.
- Controlling the speed effect of high-speed train on the results of the bridge in two-way passing with different direction mode and speeds and determining the critical speeds.
- Controlling the speed effect of high-speed train on the results of the bridge in two-way passing with different direction and speeds mode and determining the critical speeds.

The evaluation process based on these assumptions and objectives is shown in Fig. 1.

3. Bridge and train characteristics

Yan *et al.* (2015) investigated the dispersion of structural system as well as the length of high-speed railway bridges in the countries with this technology, including China, Japan, France, Germany, Spain, and Italy. According to this study, the bridge structure in high-speed railway mainly adopts simply-supported PC box-girders, as

such only on the Shanghai-Beijing HSR of China, 90% of the bridges are this type.

The studied bridge is a simply-supported concrete box girder with the span length of 24.6 m. and 28 spans. Xia *et al.* (2005) recorded the values of acceleration and displacement in spans 22 and 23 of bridge subjected to high-speed trains with different speeds using the installed sensors. This two-lane bridge superstructure is a concrete slab and bridge located in Qin-Shen high-speed railway in China. An image of the bridge cross section is presented in Fig. 2.

Based on the field study conducted on the case study bridge (Xia *et al.* 2005), the selected train for the present study is the China-Star high-speed train. In the validation stage, the train consists of two locomotives and nine wagons, and in the sensitivity analysis, the train consists of one locomotive and two wagons. The axle loads of locomotive and wagon are 19.5 and 14.25 tons, respectively. Dimensions and mechanical properties of the train car (27-DOFs dynamic system) are described in Fig. 3 and Table 1.

In the prepared FE model, shell elements are used to model concrete box girder, while concrete slab-track and

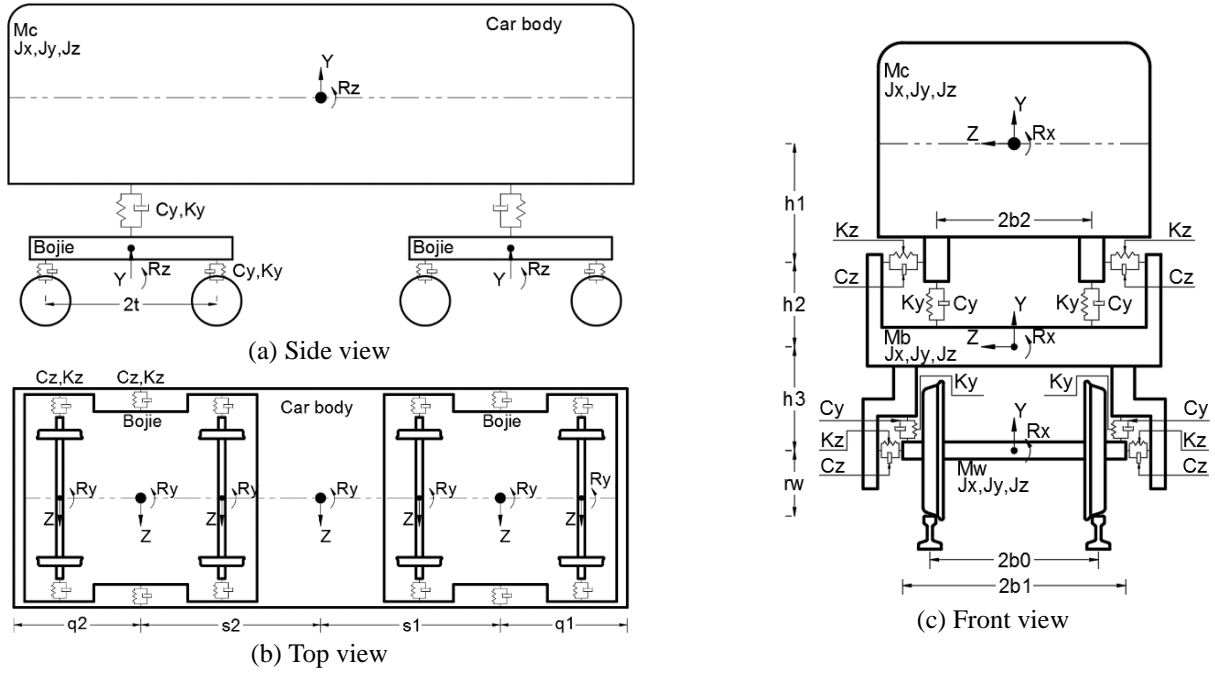


Fig. 3 Model, dimensions, and parameters of a train's car

Table 1 Mechanical properties and dimensions of an independent train car

Description	Name	Unit	Power car	Passenger cars
Car-body dimensions	s1; s2; q1; q2; h1	m	5.73;5.73;6.8;3.75;0.75	9;9;3.75;3.75;0.75
Mass of car-body	Mc	ton	63.98	43.82
Car-body inertia moments	Jx; Jy; Jz	ton.m ²	59.40, 2505.3, 2485.4	23.20, 2100.0, 2080.0
Mass of bogie	Mb	ton	3.434	3.04
Bogie inertia moments	Jx; Jy; Jz	ton.m ²	1.766, 2.453, 4.905	1.580, 2.344, 3.934
Secondary suspension stiffness	Kz; Ky	KN/m	297.2, 1245.87	176.0, 265.0
Secondary suspension damping	Cz; Cy	KNS/m	98.1, 98.1	39.2, 45.12
Secondary suspension dimensions	b2; h2	m	1.23, 0.42	1.23, 0.42
Primary suspension stiffness	Kz; Ky	KN/m	2452.5, 1226.25	2350.0, 590.0
Primary suspension damping	Cz; Cy	KNS/m	98.10, 29.43	58.86, 19.62
Mass of wheel-axle	Mw	ton	1.776	1.776
Wheel-axle moment	Jx; Jy; Jz	ton.m ²	1.138, 1.138, 0.00785	1.138, 1.138, 0.00785
Primary suspension & wheel	b0; b1; h3; t; rw	m	0.75, 1.0, 0.2, 1.25, 0.455	0.75, 1.0, 0.2, 1.25, 0.455

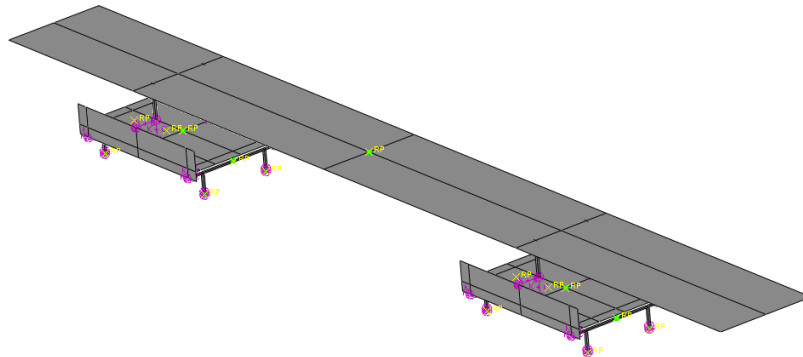


Fig. 4 Vehicle modeling

rails are modeled by solid elements. Wagons, bogies and axles are modeled by shell elements, considering discrete rigid properties and rotational inertia characteristics.

Connections are modeled using springs and viscous dampers. Wheel-rail interaction is also modeled employing Hertz-spring. An illustration of the Vehicle FE model is

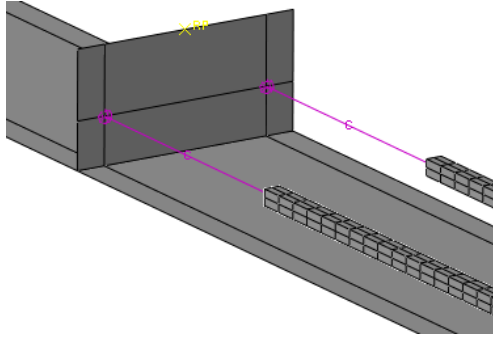


Fig. 5 Absorbent boundaries model

shown in Fig. 4.

3.1 Material damping model

The Rayleigh damping method is used to model the bridge inherent damping material. According to the field test results, the damping ratio of the bridge is calculated as 2.5% (Xia *et al.* 2005). Thus

$$[C] = \alpha[M] + \beta[K] \quad (1)$$

$$\xi_n = \frac{\alpha}{2\omega_n} + \frac{\beta\omega_n}{2} \quad (2)$$

$$\begin{Bmatrix} \alpha \\ \beta \end{Bmatrix} = \frac{2\xi}{\omega_1 + \omega_2} \begin{Bmatrix} \omega_1 \\ \omega_2 \end{Bmatrix} \quad (3)$$

In which $[C]$, $[M]$, and $[K]$ are damping, mass, and stiffness matrixes of the material, respectively. Moreover, α and β are damping coefficients, which are proportional to mass and stiffness, ξ is damping ratio, and ω_1 and ω_2 are natural frequency.

3.2 Absorbent boundaries

Because of the limited length of rails in FEM, the absorbent boundaries are modeled to absorb the incident waves at the end of the rails and prevent them from returning. In this research, the employed absorbed boundaries are speed-dependent viscose damper type suggested by Lysmer and Kuhlemeyer (1969) for solving dynamical problems.

The constants of damper per unit area in the vertical directions to the surface are obtained from the following equations

$$C_n = \rho V_p \quad (4)$$

$$V_p = \frac{3.4V_s}{\pi(1-\nu)} \quad (5)$$

Where ρ is mass per unit volume, V_p is P -wave speed, C_n is a constant of per unit area in the vertical direction to the surface, and V_s is shear wave speed. The absorbent boundaries model is shown in Fig. 5.

3.3 Boundary condition

In some research projects (Sua *et al.* 2010 and Dinh *et al.* 2009), to simplify the calculation, it was assumed that the output and input of the span had zero displacements with respect to the bridge. In the present study, to evaluate the effects of input and output of the studied span, two additional side-spans are modeled before and after the considered span, as shown in Fig. 6.

4. Modal analysis and optimization of meshing dimensions

Mesh size is one of the parameters effective on FEM analyses. Although smaller elements lead to a higher precision of the model, they require more time to analyze. In this research, modal analysis is carried out with various mesh sizes on the bridge model to determine the optimum meshing dimensions, and the calculated modal frequencies are listed in Table 2.

As shown in Table 2, the natural frequencies of the first four modes converge and do not experience any changes by decreasing the mesh sizes from 20 to 15 cm. Therefore, the

Table 2 Modal frequency results

Max mesh size(cm)	Frequency (1/sec)			
	1 th Mode	2 th Mode	3 th Mode	4 th Mode
100	7.94	11.09	19.02	20.08
75	7.86	11.11	18.97	20.01
50	7.97	11.11	18.93	19.92
30	7.72	11.1	18.94	19.84
25	7.71	11.1	18.89	19.84
20	7.68	11.09	18.88	19.82
15	7.68	11.09	18.88	19.81



Fig. 6 The main and additional side-spans of the bridge model

Table 3 A comparison between modal frequencies in FEM modeling and field test

Span	Modal frequency(Hz)	
	Field test	FEM
22th	7.65	7.68
23th	7.70	

optimal mesh size is selected as 15 cm during the analyses. The first four mode-shapes with the mesh size of 15 cm are presented in Fig. 7.

5. Verification of numerical model

In this section, the numerical model is verified using the results of the field test. The verification is based on the results of modal analysis as well as the results of the time history of displacement in the bridge middle span subjected to a high-speed China-Star train passing with a speed of 260 km/h. The train used in the validation selected based on the passing train in the field test (Xia *et al.* 2005), consists of two locomotives and nine wagons, with the axle load of the locomotive and wagons being 19 ton 14.5 ton, respectively. A comparison between modal frequencies in FEM and field test is presented in Table 3. As shown in Table 3, the results of the first modal frequency in the FEM completely match to modal frequencies of the field test.

A comparison between the displacements at the mid-span in FEM and field test is shown in Fig. 8.

As seen from Fig. 8, the results of this part completely match those of the field tests; suggesting the modeling behavior accuracy of the prepared FEM.

6. Results of sensitivity analysis

After proving the behavior accuracy and the results of FEM, the results of sensitivity analysis are presented in this section. The dynamical responses of the bridge under a high-speed train in various passing scenarios are demonstrated through the one-way passing, two-way passing in different directions at same speeds, and two-way passing in different directions at different speeds.

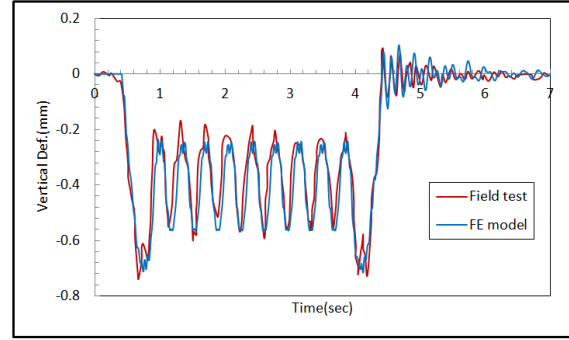


Fig. 8 Displacement time histories of mid-span obtained by numerical model and field tests, for a train speed of 260 km/h

One of the most important parameters in the analysis of dynamic issues is excitation frequency. According to the passing speeds and loading intervals, the excitation frequency value is calculated by the following equation:

$$f = \frac{V}{S} \quad (6)$$

Where V is passing speed and S is the distance between loading points. The excitation frequencies of the train considered are shown in Table 4.

The results of displacement and acceleration in different points of the bridge such as bridge mid-span and a bridge quarter-span are recorded in Fig. 9. PL and PR represent the left and right entrances of the span, respectively. PM indicates points in the middle of the span, while those marked by PSL and PSR represent points in left and right quarter of the span, respectively. Moreover, PL, PSL3, PM3, PSR3, and PR are located in center-line of the span.

6.1 The results of one-way passing mode

For this mode, the results of acceleration and displacement in different points of the bridge under a high-speed train moving at speeds of 120 to 350 km/h are presented. The FE model of bridge and train in one-way passing mode are presented in Fig. 10. It is noteworthy that train moves across the bridge from the side that marked with PL to the side that marked with PR.

Table 4 The excitation frequencies of passing train at various speeds

V (km/h)	V (m/sec)	Power car		Passenger cars	
		Axles inv(m)	Bojvie inv(m)	Axles inv(m)	Bojvie inv(m)
		3	11.46	2.56	18
		Frequency(Hz)		Frequency(Hz)	
120	33.3	11.11	2.91	13.02	1.85
150	41.7	13.89	3.64	16.28	2.31
180	50.0	16.67	4.36	19.53	2.78
220	61.1	20.37	5.33	23.87	3.40
260	72.2	24.07	6.30	28.21	4.01
300	83.3	27.78	7.27	32.55	4.63
350	97.2	32.41	8.48	37.98	5.40

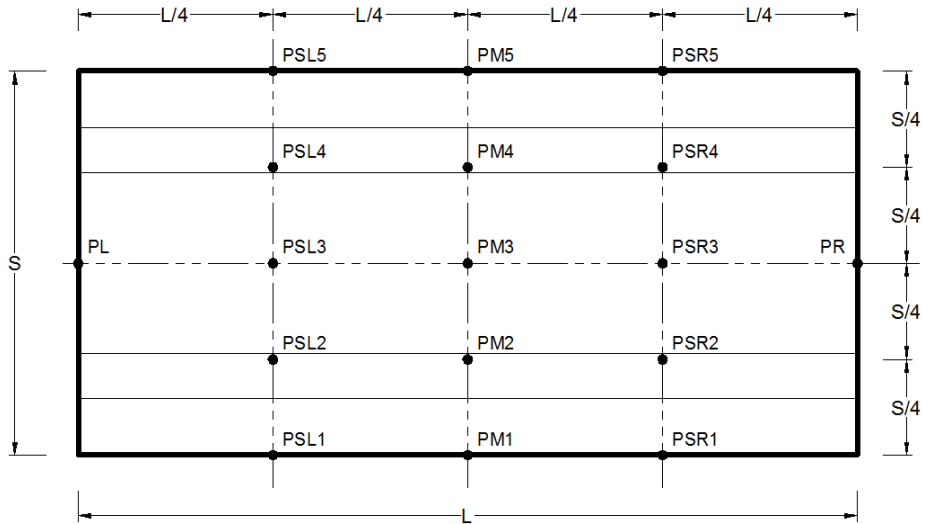
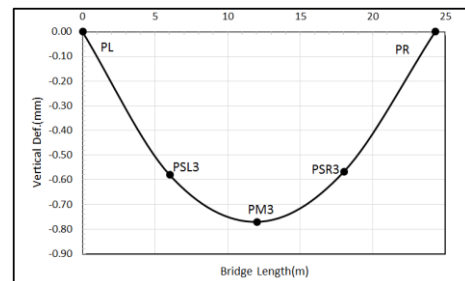


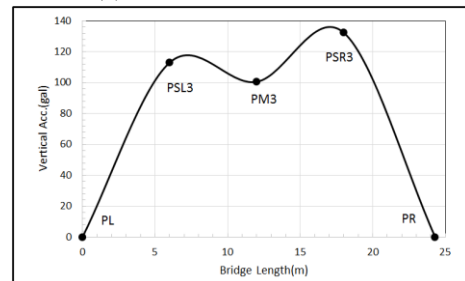
Fig. 9 The target record points in the bridge deck



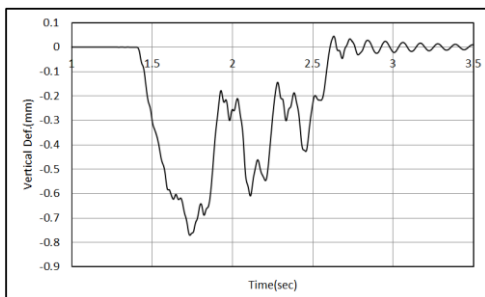
Fig. 10 3D FE model of one-way passing mode



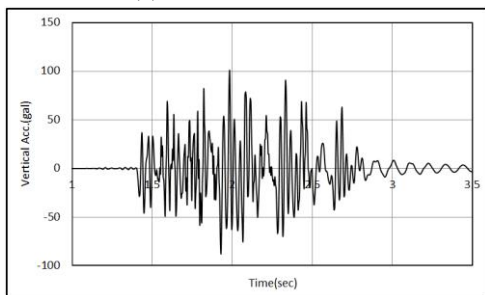
(a) Max. Vertical deflection



(b) Max. Vertical acceleration



(a) Vertical deflection



(b) Vertical acceleration

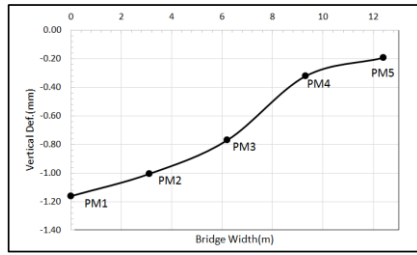
Fig. 11 The acceleration and deflection time histories of the bridge at mid-span (PM3) under train speed of 260 km/h (One way passing)

Fig. 12 The maximum vertical deflections and accelerations of the bridge at the center-line of the span under train speed of 260 km/h (One way passing)

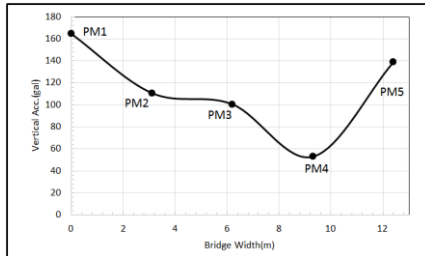
shown in Figs. 11-14 as a passing speed sample.

As shown in Fig. 12, the maximum displacement occurs at bridge mid-span, while the maximum acceleration occurs at the quarter-span. Moreover, as seen in Fig. 13, in the one-way passing mode the torsion occurs at both sides of the bridge deck and shows an approximately 6 times displacement difference, while the maximum acceleration occurs at the bridge side-line on the passing side (PM1). Based on Fig. 14, the acceleration and displacement in entrance and exit sides of the bridge quarter-span crossbeam are almost identical. In addition, the maximum displacement occurs at the bridge side-line on passing side and the bridge side-line on the other side is uplifted. The maximum displacements and accelerations at bridge mid-span and middle crossbeam (PM1 and PM5) under various

The calculated results of acceleration and displacement at mid-span (PM3), the center-line of the span, and the mid-span crossbeam under the train speed of 260 km/h are

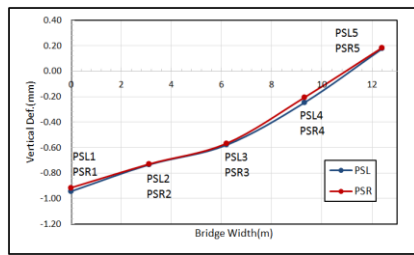


(a) Max. Vertical deflection

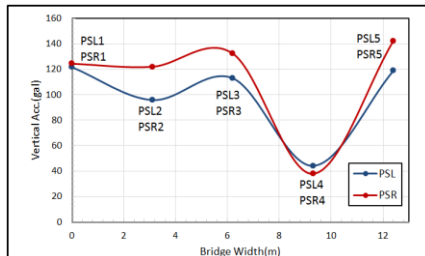


(b) Max. Vertical acceleration

Fig. 13 The maximum vertical deflections and accelerations of the bridge at mid-span crossbeam under train speed of 260 km/h (One way passing)



(a) Max. Vertical deflection



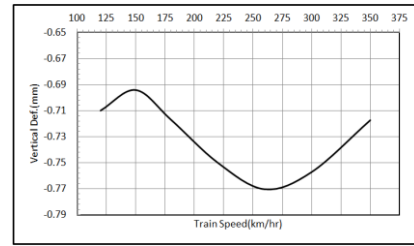
(b) Max. Vertical acceleration

Fig. 14 The maximum vertical deflections and accelerations of the bridge at quarter-span crossbeam under train speed of 260 km/h (One way passing)

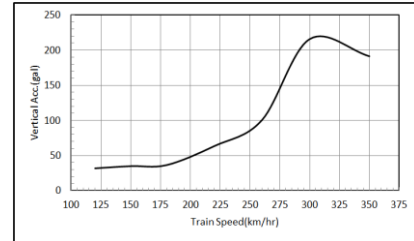
train speeds are presented in Figs. 15 and 16.

As presented in Fig. 15, the maximum displacement occurs at speeds of 260 to 300 km/h, wherein the excitation frequencies related to the train axles and bogies are close to the natural frequencies of bridge. Moreover, it is evident that the displacement of bridge mid-span at speed of 120 km/h has a peak value too and the maximum acceleration occurs at speed of 300 km/h. In this mode, as presented in Fig. 16 the bridge experiences torsion but acceleration in the bridge side-crossbeams are identical.

6.2 Results of the two-way passing mode at same train speeds

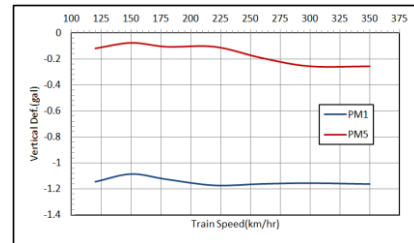


(a) Max. Vertical deflection

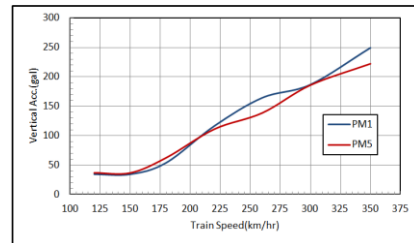


(b) Max. Vertical acceleration

Fig. 15 The results of mid-pan at different passing speeds(PM3)



(a) Max. Vertical deflection



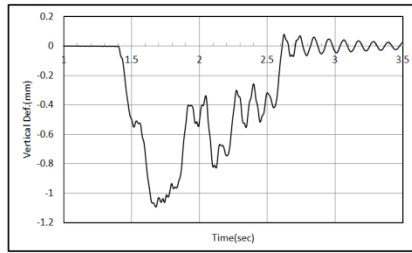
(b) Max. Vertical acceleration

Fig. 16 The results of span middle crossbeam at different passing speeds(PM1&PM5)

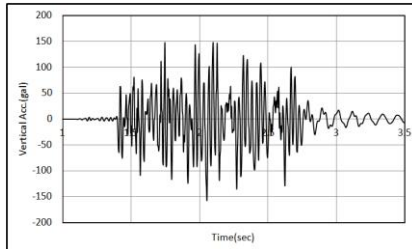


Fig. 17 The 3D FE model of two-way train passing mode

In this mode, the results of acceleration and displacement are presented at various points of the bridge subjected to parallel train passing in opposite directions but

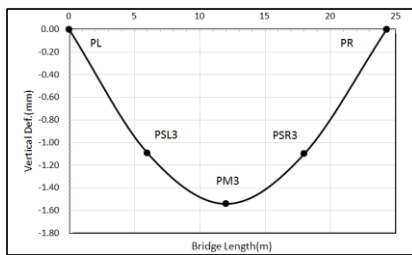


(a) Vertical deflection

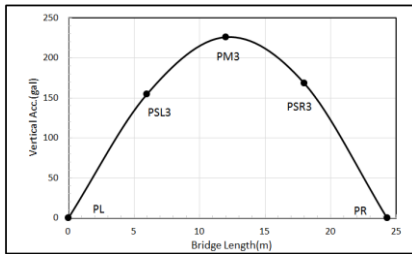


(b) Vertical acceleration

Fig. 18 The acceleration and deflection time histories of the bridge at mid-span (PM3) under train speed of 260 km/h (two-way passing in different directions at same speeds)



(a) Max. Vertical deflection



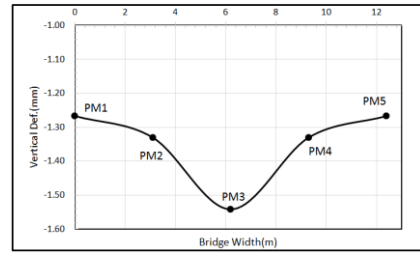
(b) Max. Vertical acceleration

Fig. 19 The maximum vertical deflections and accelerations of the bridge at center-line of span under train speed of 260 km/h (two-way passing in different directions at same speeds)

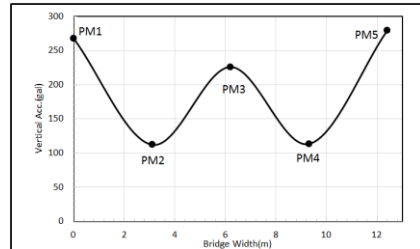
at the same speeds. The bridge and two-way passing train FE model are shown in Fig. 17.

Same as the previous mode, the results of acceleration and displacement in different points such as the bridge mid span (PM3), the bridge center-line of span, and the bridge middle crossbeam at the passing speed of 260 km/h are presented in Figs. 18-21 as a passing speed sample.

In this mode, according to Fig. 19, the maximum displacement and acceleration occur at the mid-span of the bridge. Moreover, in the two-way passing mode, the maximum displacement occurs in bridge middle crossbeam (PM3) and the maximum acceleration occurs in bridge crossbeam side points (PM1 and PM5) and the middle part

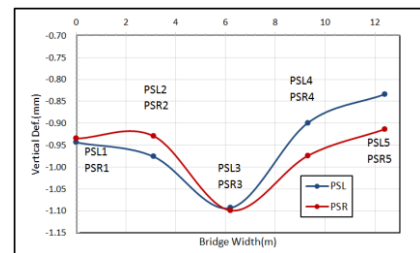


(a) Max. Vertical deflection

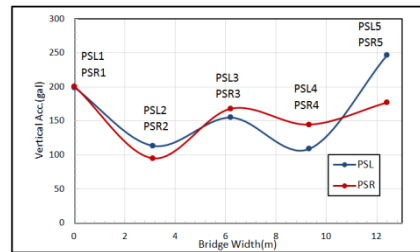


(b) Max. Vertical acceleration

Fig. 20 The maximum vertical deflections and accelerations of the bridge at mid-span crossbeam under train speed of 260 km/h (two-way passing in different directions at same speeds)



(a) Max. Vertical deflection



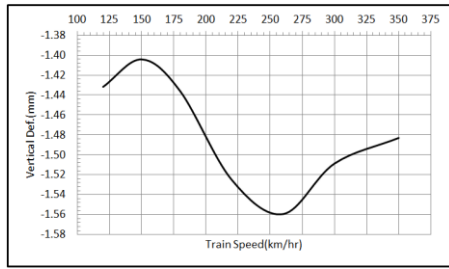
(b) Max. Vertical acceleration

Fig. 21 The maximum vertical deflections and accelerations of the bridge at quarter-span crossbeam under train speed of 260 km/h (two-way passing in different directions at same speeds)

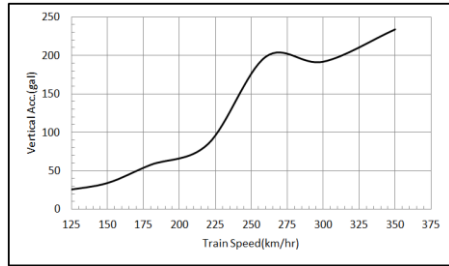
of the bridge (PM3), which are shown in Figs. 20 and 21.

The maximum displacement and acceleration in the bridge mid-span and middle crossbeam (PM1 and PM5) at various speeds are presented in Figs. 22 and 23.

In this mode, the maximum displacement occurs at speeds of 260 km/h (Fig. 22). Due to the proximity of train excitation frequency to natural frequency of bridge, the maximum acceleration has an ascending trend up to a speed of 350 km/h, but being steady at 260 km/h. In this mode, the bridge experiences no torsion and the displacement and acceleration in the bridge side-crossbeams are identical (Fig. 23). Comparing Figs. 15 and 22 shows that the

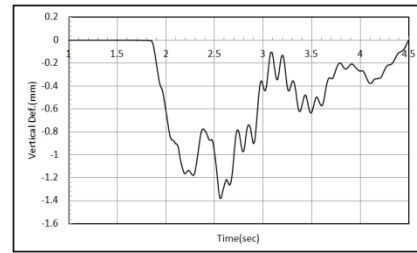


(a) Max. Vertical deflection

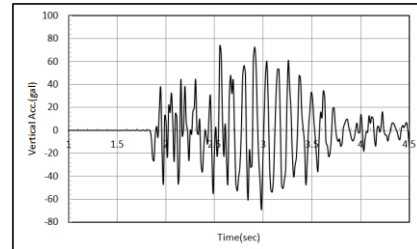


(b) Max. Vertical acceleration

Fig. 22 The results of mid-span at different passing speeds (PM3)

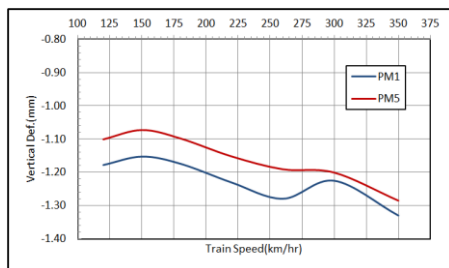


(a) Vertical deflection

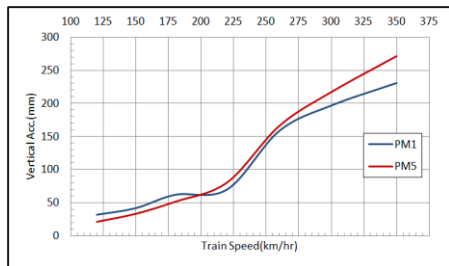


(b) Vertical acceleration

Fig. 24 The acceleration and deflection time histories of the bridge at mid-span (PM3) under trains parallel passing in an opposite direction at speeds of 120 km/h and 260 km/h

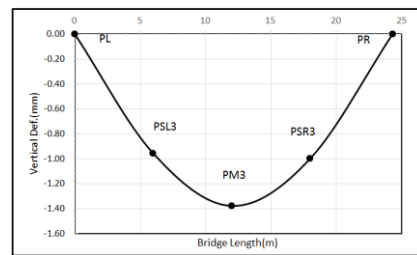


(a) Max. Vertical deflection

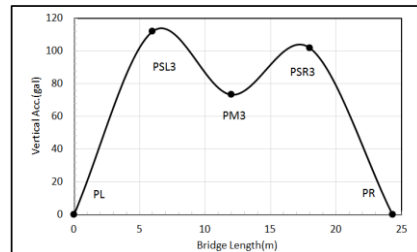


(b) Max. Vertical acceleration

Fig. 23 The results of span middle crossbeam at different passing speeds (PM1 & PM5)



(a) Max. Vertical deflection



(b) Max. Vertical acceleration

Fig. 25 The maximum vertical deflections and accelerations of the bridge at center-line of span under trains parallel passing in an opposite direction at speeds of 120 km/h and 260 km/h

maximum displacement in this scenario is twice that of one-way passing scenario. However, maximum accelerations in both scenarios are the same.

6.3 Results of two-way passing mode at different train speeds

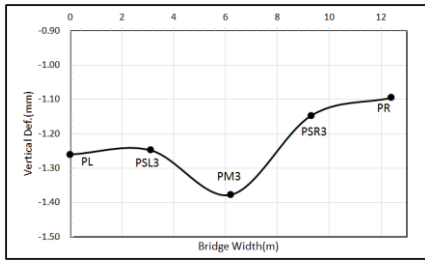
In this mode, the results of acceleration and displacement are presented at various points of the bridge subjected to parallel train passing in opposite directions but at different speeds. In this mode, the train passing from *L* has a speed of 120 km/h and other trains passing from *R* have the speeds of 120 to 350 km/h.

Similar to the previous mode, first, the results of

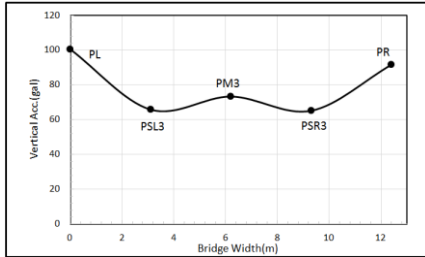
acceleration and displacement in different points such as the bridge mid-span, the bridge middle longitudinal girder, and the bridge middle crossbeam subjected to the passing trains from *L* and *R* at the passing speed of 120 km/h and 260 km/h, are presented in Figs. 24-27.

In this mode, the maximum displacement occurs in the mid-span of the bridge, but unlike the previous mode, the maximum acceleration occurs in quarter-span and acceleration in the bridge quarter-span is not the same on the both sides (Fig. 25).

The maximum displacement and acceleration in the bridge mid-span and middle crossbeam (PM1 and PM5) at various speeds are presented in Figs. 28 and 29.

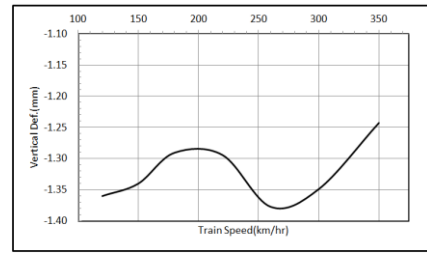


(a) Max. Vertical deflection

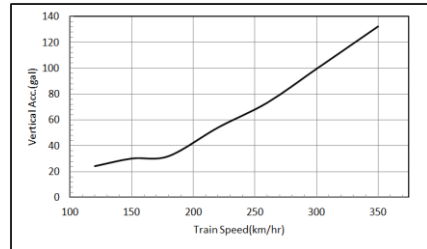


(b) Max. Vertical acceleration

Fig. 26 The maximum vertical deflections and accelerations of the bridge at mid-span crossbeam under trains parallel passing in an opposite direction at speeds of 120 km/h and 260 km/h

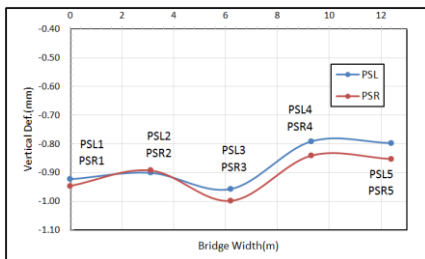


(a) Max. Vertical deflection

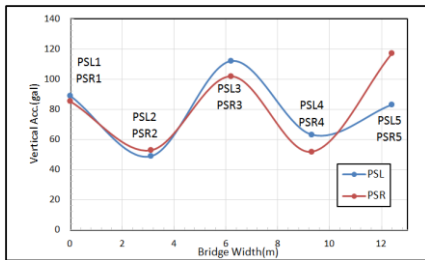


(b) Max. Vertical acceleration

Fig. 28 The results of mid-span (PM3) at different passing speeds under trains parallel passing in an opposite direction

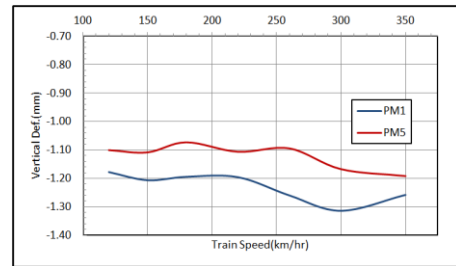


(a) Max. Vertical deflection

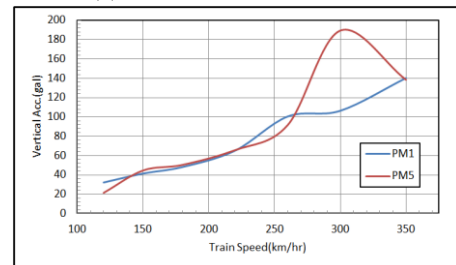


(b) Max. Vertical acceleration

Fig. 27 The maximum vertical deflections and accelerations of the bridge at quarter-span crossbeam under trains parallel passing in an opposite direction at speeds of 120 km/h and 260 km/h



(a) Max. Vertical deflection



(b) Max. Vertical acceleration

Fig. 29 The results of span middle crossbeam at different passing speeds(PM1&PM5) under trains parallel passing in an opposite direction

experiences small torsion in this mode.

7. Conclusions

This research was conducted to investigate the response of a two-lane bridge subjected to high-speed train in different passing modes such as one-way passing, two-way passing in opposite direction and same speeds, and two-way passing in opposite direction at different speeds. A FE model was presented to simulate the train-bridge interaction and the field test results carried out by Xia *et al.* (2005) were adopted to validate the model.

The results show that in the one-way passing mode, the

According to Fig. 28 the maximum displacement occurs under two passing train at speeds of 120 and 260 km/h, due to the proximity of excitation frequencies to the natural frequency of bridge in both speeds. The other maximum displacement occurs when the passing speed for both trains is the same (120 km/h). This issue is important because train passage at speeds much less than the maximum passing speeds can be critical to the bridge. In this mode, the maximum acceleration has an ascending trend by an increase of train speed, but still drastically low compared to the value of previous modes. As seen in Fig. 29, the bridge

points of maximum acceleration and displacement values are not the same on the bridge; i.e., the maximum displacement occurs at bridge mid-span while the maximum acceleration at the quarter-span. In this mode, the bridge experiences a torsion, but the acceleration is same on the both sides of the deck. In addition, displacement and acceleration values are almost identical in entrance and exit of quarter-span. Another result in this mode is the critical speed corresponding to the displacement and acceleration that is equal to 260 to 300 km/h. At this speed range, the loading frequency is near the natural frequency of bridge system. It is also found that the displacement of bridge mid-span at speed of 120 km/h has a peak value too.

In the two-way passing mode with opposite direction and the same speed, the maximum acceleration and displacement occur in bridge mid-span. It is also found that the critical speed in the control of displacement is 260 km/h. However, the displacement at speed of 120 km/h is the maximum too, but due to the proximity of excitation frequency and natural frequency of the bridge, the maximum acceleration shows an ascending trend by increasing the speed and 260 km/h is the maximum point for acceleration. Therefore, the acceleration and displacement at a particular passing speed, wherein the loading frequency is close to natural frequency, will be the maximum. Hereby, the maximum displacement in two-way passing mode at same speeds and opposite direction is twice more than one-way passing mode, but the maximum acceleration in both modes is almost identical.

In two-way passing mode at a different speed and opposite direction, the maximum displacement occurs in trains passing at a speed of 120 and 260 km/h, due to the proximity of the excitation frequencies and bridge modal frequency at these passing speeds. Besides, the maximum displacement occurs at a passing speed of 120 km/h for both trains too. This issue is rather important, since train passing at speeds way less than the maximum operational speeds of high-speed trains could result in excitation of the bridge. The maximum displacement in this passing mode is less than that of the parallel passing mode at the same speed while it is more than that of one-way passing (about 88% of parallel passing mode at the same speed and 77% more than one-way passing mode). The acceleration in this passing mode has an ascending trend by increasing the passing speeds, but the value is less compared with that of the previous mode.

Acknowledgments

This research has been supported by railway Engineering Department and Research and Technology Affairs of Iran University of Science and Technology. Authors wish to thank gratefully this support mode.

References

Adam, C. and Salcher, P. (2014), "Dynamic effect of high-speed trains on simple bridge structures", *Struct. Eng. Mech.*, **51**(4), 581-599.

- Bhaskar, A., Johnson, K.L., Wood, G.D. and Woodhouse, G. (1997), "Wheel-rail dynamics with closely conformal contact, Part 1: dynamic modelling and stability analysis", *Instn. Mech. Eng.*, **211**(F1), 11-27.
- Delgado, R.M. and Santos, S.M. (1997), "Modelling of railway bridge-vehicle interaction on high speed tracks", *Comput. Struct.*, **63**(3), 511-523.
- Dinh, V.N., Kim, K.D. and Warnitchai, P. (2009), "Dynamic analysis of three-dimensional bridge-high-speed train interactions using a wheel_rail contact model", *Eng. Struct.*, **31**, 3090-3106.
- Dinh, V.N., Kim, K.D. and Warnitchai, P. (2009), "Simulation procedure for vehicle-substructure dynamic interactions and wheel movements using linearized wheel-rail interfaces", *FE. Analy. Des.*, **45**, 341-456.
- Inglis (1934), *Mathematical Treatise on Vibration in Railway Bridges*, The University Press, Cambridge, UK
- Li, Z, Li, S, Lv, H. and Li, H. (2015), "Condition assessment for high speed railway bridge based on train induced strain response", *Struct. Eng. Mech.*, **54**(2), 199-219.
- Liu, K., DeRoeck, G. and Lombaert, G. (2009), "The effect of dynamic train-bridge interaction on the bridge response during a train passage", *J. Sound Vib.*, **325**, 240-251.
- Lysmer, J. and Kuhlemeyer R.L. (1969), "Finite dynamic model for infinite media", *J. Eng. Mech. Div.*, **95**(4), 859-877.
- Naëimi, M., Zakeri, J.A., Esmaili, M. and Shadfar, M. (2014), "Influence of uneven rail irregularities on the dynamic response of the railway track using a three-dimensional model of the vehicle-track system", *Veh. Syst. Dyn.*, **53**(1), 88-111.
- Podworna, M. (2014), "Vibrations of bridge / track structure / high-speed train system with vertical irregularities of the railway track", *Proc. Eng.*, **91**, 148 - 153.
- Sua, D., Fujino, Y., Nagayama, T., Hernandez, J. and Sekic, M. (2010), "Vibration of reinforced concrete viaducts under high-speed train passage: measurement and prediction including train-viaduct interaction", *Struct. Infrastr. Eng.*, **6**(5), 621-633.
- Ugarte, J., Carnerero, A. and Millanes, F. (2017), "Dynamic behavior of pergola bridge deck of high speed railways", *Struct. Eng. Mech.*, **61**(1), 91-103.
- Vesali, F., Rezvani, M.A. and Eghbali, A. (2013), "Dynamic response of railway bridges traversed simultaneously by opposing moving trains", *Struct. Eng. Mech.*, **46**(5), 713-734.
- Wu, J.S. and Dai, C.W. (1987), "Dynamic responses of multi-span non-uniform beam due to moving loads", *J. Struct. Eng.*, **113**(3), 458-474.
- Xia, C.Y., Lei, J.Q., Zhang, N., Xia, H. and Roeck, G. (2012), "Dynamic analysis of a coupled high-speed train and bridge system subjected to collision load", *J. Sound Vib.*, **331**, 2334-2347.
- Xia, C.Y., Xia, H. and Roeck, G. (2014), "Dynamic response of a train-bridge system under collision loads and running safety evaluation of high-speed trains", *Comput. Struct.*, **140**, 23-38.
- Xia, H. and Zhang, N. (2005), "Dynamic analysis of railway bridge under high-speed trains", *Comput. Struct.*, **83**, 1891-1901.
- Xia, H., Xu, Y.L., Chan, T.H.T. and Zakeri, J.A. (2007), "Dynamic response of railway suspension bridge under moving trains", *J. Scien. Iran.*, **14**(5), 385-394.
- Xia, H., Zhang, N. and Gao, R. (2005), "Experimental analysis of railway bridge under high-speed trains", *J. Sound Vib.*, **282**, 517-528.
- Yan, B., Dai, G.L. and Hu, N. (2015), "Recent development of design and construction of short span high-speed railway bridges in China", *Eng. Struct.*, **100**, 707-717.